Molecular Structure and Infrared Spectra of 4-Fluorophenol: A Combined Theoretical and Spectroscopic Study

Wiktor Zierkiewicz* and Danuta Michalska

Institute of Inorganic Chemistry, Wrocław University of Technology, Wybrzeże Wyspiańskiego 27, 50-370 Wrocław, Poland

Bogusława Czarnik-Matusewicz and Maria Rospenk

Faculty of Chemistry, University of Wrocław, Joliot-Curie 14, 50−383 Wrocław, Poland

Received: December 9, 2002; In Final Form: March 14, 2003

The molecular structure of *para*-fluorophenol (*p*-FPhOH) has been calculated using the MP2 and density functional (B3LYP) methods with the extended 6-311++G(df,pd) basis set. The gas-phase structure of this molecule has not been reported, as yet. For the series of phenols, *p*-XPhOH (X = H, F, Cl, Br), the calculated geometrical parameters and natural atomic charges are compared and discussed. It is shown that in *para*-fluorophenol, the structural changes of the ring are governed chiefly by the electronegativity of fluorine (inductive effect). However, resonance effects induced by the OH and F substituents in the *para* position also contribute to the geometrical changes of the aromatic ring. The FT-IR spectra of *p*-fluorophenol and its OD-deuterated derivative (*p*-FPhOD) in carbon tetrachloride and cyclohexane solutions were measured, in the frequency range 3700−400 cm^{-1}, and the experimental integrated infrared intensities were determined. The harmonic frequencies and IR intensities of *p*-FPhOH and *p*-FPhOD were calculated with the B3LYP method using the 6-311++G(df,pd) basis set. The unequivocal assignment of the experimental spectra has been made on the basis of the calculated potential energy distribution, PED. The characteristic "marker" IR bands for phenol and its *para*-halogeno derivatives are discussed. The unusual quenching of the infrared intensities of several bands in the spectra of *p*-fluorophenol has been explained.

Introduction

In the past few years, a number of theoretical and experimental studies have been reported on the infrared spectra of phenol and its radical cation.[1−7] Recently, we have performed comprehensive spectroscopic and theoretical investigations of the molecular structures and infrared spectra of *para*-chloro- and *para*-bromophenols and their OD-deuterated derivatives.[8] In contrast, only scarce information is available for *para*-fluorophenol. Cabana et al.[9] determined the frequencies and infrared intensities of the OH stretching vibrations in halophenols (including *para*-fluorophenol). Larsen and Nicolaisen[10] reported a few bands in the far-infrared spectra of *p*-FPhOH in the vapor phase. The frequencies of *p*-fluorophenol in the range 1600−400 cm^{-1} have been reported;[11,12] nevertheless, their assignment is still uncertain and contradictory. Moreover, the molecular structure of *p*-fluorophenol in the gas phase has not been determined, as yet.

It should be noted that much more information is available on *ortho*-fluorophenol. Recently, Hargittai and co-workers[13,14] and other authors[15,16] reported electron diffraction studies and theoretical calculations on 2-fluorophenol and 2,6-difluorophenol. Tishchenko et al.[17] performed extensive theoretical vibrational analysis of the series of monohalogenated phenols.

The hydrogen-bonded complexes of *p*-FPhOH with *N*-oxides have been studied with IR spectroscopy and revealed an interesting continuum in their absorption.[18] The formation constants have been reported for the hydrogen-bonded complexes between *p*-FPhOH and several halogenoalkanes.[19]

The unequivocal assignment of the bands in the infrared spectrum of a bare *para*-fluorophenol is indispensable for a clear understanding of the spectral changes in the hydrogen-bonded complexes and clusters. The stretching and bending vibrations of the O−H and C−F groups in *p*-FPhOH are sensitive to intermolecular interaction. By monitoring the frequency shifts of these modes in the infrared spectra, it is possible to provide direct information on the H-bond interaction in larger systems.

Therefore, in the present work we have undertaken a thorough theoretical study of the molecular structure, natural atomic charges, vibrational frequencies, and integrated IR intensities of *p*-fluorophenol and its OD-deuterated derivative, using the second-order Möller−Plesset (MP2) and density functional (DFT/B3LYP) methods with the extended 6-311++G(df,pd) basis set. These calculations were complemented by the experimental study of the infrared spectra of *p*-FPhOH and *p*-FPhOD in inert solvents. The integrated IR intensities have not been reported for these molecules, until now. The clear-cut assignment of all the bands in the experimental spectra has been made on the basis of the calculated potential energy distribution, PED.

The second purpose of this work is the detailed theoretical investigation of the substituent effects in the series of *para*-halophenols (*p*-XPhOH, X = F, Cl, and Br). This study may shed more light on the changes in geometrical parameters and charge distribution in the benzene ring caused by the two para-substituents, the OH group and the halogen atom.

Methods

Theoretical. The geometry optimization of *para*-fluorophenol has been performed using the ab initio MP2 method[20] and

* Corresponding author, e-mail: wiktor@ichn.ch.pwr.wroc.pl

10.1021/jp022564q CCC: $25.00
Published on Web 05/10/2003

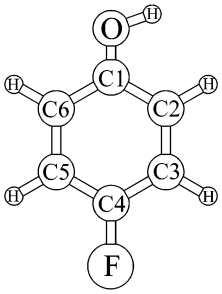

Figure 1. Atom numbering in *para*-fluorophenol.

the density functional three-parameter hybrid model (DFT/B3LYP).[21,22] In all calculations the 6-311++G(df,pd) basis set has been employed.[23,24] This is the valence triple-ζ basis set, augmented by d,f-polarization functions on carbon and oxygen atoms; p,d-polarization functions on hydrogen atoms; and enlarged by diffuse functions on all atoms. For the series of phenols *p*-XPhOH (X = H, F, Cl, Br), a natural bond orbital (NBO) analysis[25] has been performed with both the MP2 and B3LYP electron densities. The harmonic frequencies and infrared intensities of *para*-fluorophenol and its OD-deuterated derivative have been calculated at the B3LYP/6-311++G(df,-pd) level. In our earlier studies[1a,8] we have demonstrated that this level of theory gives excellent results in predicting vibrational spectra of phenol, *p*-chlorophenol, and *p*-bromophenol, whereas the MP2 method is deficient for certain modes in aromatic molecules. The scaling factor for the calculated frequencies of phenols (below 2000 cm^{-1}) has been determined previously.[8] The B3LYP-calculated frequencies of the CH and OH(OD) stretching vibrations were scaled using a scale factor derived by Baker et al.[26] The nonredundant set of 33 internal coordinates has been used as recommended by Fogarasi and Pulay.[27] The normal coordinate analysis has been carried out for both the molecules, according to the procedure described in our earlier papers.[28,29] The calculated potential energy distributions (PEDs) for *p*-FPhOH and *p*-FPhOD have enabled us to make detailed assignments of the experimental IR spectra of these molecules. The symmetry coordinates for the six-membered ring are given in ref 29. All calculations have been performed with the Gaussian 98 package.[30]

Experimental. The FT-IR spectra of *p*-FPhOH and *p*-FPhOD in carbon tetrachloride (3700−850 cm^{-1}) and in cyclohexane (850−400 cm^{-1}) solutions at a concentration of 0.05 mol dm^{-3} were recorded at room temperature. The spectra were measured at 0.5 cm^{-1} resolution on a Nicolet Magna System 860 spectrometer equipped with a KBr beam splitter, a Globar source, and a DTGS detector, using a KBr liquid cell. The integrated intensities were determined, and overlapping bands were resolved into individual components using the GALACTIC GRAMS program.

p-Fluorophenol purchased from Merck was recrystallized from a petroleum−ether mixture. The deuterated derivative, *p*-FPhOD was prepared by several exchanges in methanol-OD (99%, Radioisotope Centre POLATOM). About 90% deuteration was achieved, as judged from the absorbance of the OH stretching band. The solvents (carbon tetrachloride and cyclohexane) purchased from Aldrich were dried on molecular sieves.

Results and Discussion

Structural Parameters. An accurate prediction of the structural parameters for *para*-fluorophenol, *p*-FPhOH, is of special interest because there are no experimental data reported for this molecule in the gas phase. Figure 1 shows the numbering of atoms in the title molecule. In Table 1 the theoretical bond lengths and bond angles optimized at the MP2/6-311++G(df,-pd) level for *p*-fluorophenol are listed along with the corresponding geometrical parameters reported in our earlier calculations for phenol[1a] and *p*-halophenols (*p*-XPhOH, X = Cl, Br).[8] Very similar results have been obtained with the B3LYP/6-311++G(df,pd) method and are given as Supporting Information.

TABLE 1: Bond Lengths (Å), Bond Angles (°), Interatomic Distances (Å), and Dipole Moments (D) of Phenol, *p*-Fluorophenol, *p*-Chlorophenol, and *p*-Bromophenol (p-XC_6H_4OH, X = H, F, Cl, Br) Calculated at the MP2/6-311++G(df,pd) Level

	X=H[a]	X=F	X=Cl[a]	X=Br[a]
C4−X	1.0840	1.3406	1.7282	1.8848
C1−O7	1.3649	1.3651	1.3636	1.3629
O7−H	0.9602	0.9600	0.9603	0.9603
C1−C2	1.3959	1.3959	1.3954	1.3956
C2−C3	1.3952	1.3958	1.3943	1.3948
C3−C4	1.3937	1.3864	1.3917	1.3927
C4−C5	1.3963	1.3890	1.3943	1.3957
C5−C6	1.3923	1.3925	1.3912	1.3915
C6−C1	1.3955	1.3961	1.3954	1.3957
C2−H	1.0869	1.0865	1.0866	1.0867
C3−H	1.0849	1.0835	1.0839	1.0839
C5−H	1.0849	1.0836	1.0840	1.0839
C6−H	1.0842	1.0840	1.0841	1.0843
C1−C2−C3	119.80	120.25	120.24	120.28
C2−C3−C4	120.40	118.87	119.65	119.55
C3−C4−C5	119.39	121.74	120.36	120.47
C4−C5−C6	120.63	119.08	119.86	119.74
C5−C6−C1	119.64	120.14	120.11	120.16
C6−C1−C2	120.14	119.08	119.78	119.80
C5−C4-X	120.34	119.12	119.82	119.78
C6−C1−O7	117.21	117.21	117.28	117.28
C1−O7−H	108.11	108.26	108.30	108.35
C3−C2−H	120.23	119.64	119.63	119.56
C5−C6−H	121.45	120.86	120.86	120.83
C4−C3−H	120.24	119.85	120.03	120.31
C4−C5−H	120.05	119.68	119.86	120.13
C1···C4	2.7939	2.7686	2.7854	2.7852
C2···C6	2.4191	2.4169	2.4142	2.4148
C3···C5	2.4087	2.4244	2.4172	2.4206
μ	1.4729	2.0777	2.2187	2.2850

[a] Comparison with some data from ref 8.

According to calculations at both levels of theory, *p*-FPhOH is planar (likewise other *p*-halophenols[8]). As shown in Table 1, the calculated C−Cl and C−Br bond lengths in *p*-chlorophenol and *p*-bromophenol are 1.7282 Å and 1.8848 Å, respectively. These results are in excellent agreement with the experimental values of 1.7204 Å and 1.8762 Å for C−Cl and C−Br atom distances, respectively, reported by Larsen[31] from the microwave (MW) study of these molecules in the gas phase. Thus, it seems that the C−F bond length of 1.3406 Å, calculated at the same level for *p*-fluorophenol, should be accurate. The B3LYP method yields the C−F distance slightly longer (by 0.0128 Å) than the MP2 calculation. For comparison, a similar value of the C−F distance, 1.354 ± 0.006 Å, has been determined in fluorobenzene vapor using microwave spectroscopy.[32] The C−F bond length in 2-fluorophenol, obtained from gas electron diffraction (ED), is also similar, r_g = 1.353 ± 0.012 Å.[13] However, it should be noted that the theoretical value refers to the r_e equilibrium distance, while the ED result corresponds to the r_g parameter, and the MW result is a partial r_s value.[33,34]

In Figure 2A the differences between the corresponding bond lengths calculated for *p*-XPhOH (X = F, Cl, Br) and phenol are compared. Figure 2B illustrates the differences between the

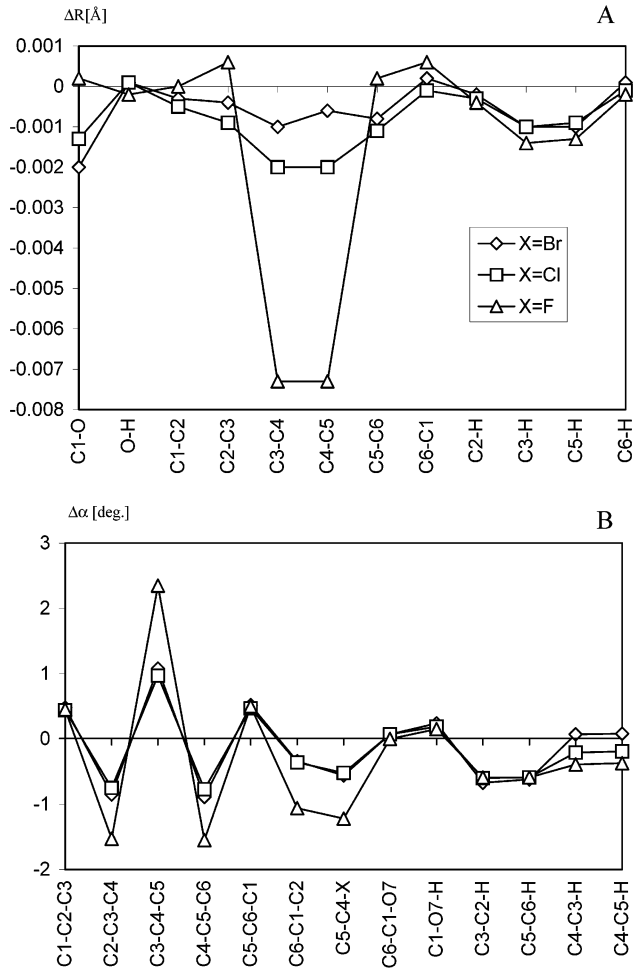

Figure 2. (A) Differences between the corresponding bond lengths (Å) in *para*-halophenols and phenol ($\Delta R = R_{XPhOH} - R_{PhOH}$). (B) Differences between the corresponding bond angles. Calculations performed at the MP2/6-311++G(df,pd) level.

corresponding bond angles in these molecules. It is evident from Figure 2A that the fluorine substituent causes the most pronounced decrease of the C_3-C_4 and C_4-C_5 bond lengths (by about 0.007 Å relative to those in phenol). A similar effect occurs in fluorobenzene, where the corresponding C−C bonds at the place of fluorine substitution are also shorter (by about 0.01 Å) than other C−C distances, as demonstrated by the MW study.[32] According to the MP2 calculations, the decrease of the C_3-C_4 and C_4-C_5 bond lengths in *p*-ClPhOH and *p*-BrPhOH is much smaller (0.002 Å and 0.001 Å, respectively).

As is seen in Figure 2A for *p*-FPhOH, the C_2-C_3, C_5-C_6, and C_6-C_1 bonds are slightly elongated in comparison to phenol. However, it is interesting to note that the opposite effect is observed in *p*-chloro- and *p*-bromophenol, where the C_2-C_3 and C_5-C_6 bonds are slightly shorter than in phenol. This indicates some contribution of the quinoid-type structure[35] in *p*-chloro- and *p*-bromophenol, but not in *p*-fluorophenol. Another bond length that evidently differs in these molecules is the C_1-O distance. It follows from Table 1 that the fluorine substituent leads to a slight elongation of the C−O bond, while the chlorine and, particularly, bromine substituents cause a shortening of this bond, with regard to phenol.

As illustrated in Figure 2B, there is considerable angular deformation in the phenol ring caused by the presence of the fluorine atom, whereas much smaller changes are observed for the chlorine and bromine substituents. In *p*-FPhOH, the $C_3-C_4-C_5$ internal ring angle increases by about 2.4°, while the adjacent two angles in the ring decrease by about 1.6° in comparison to phenol. These structural changes are consistent with the σ-electron-withdrawing (inductive) effect of the fluorine substituent.[35] It should be noted, however, that the MP2-calculated $C_3-C_4-C_5$ bond angle in *para*-fluorophenol (121.74°) is slightly smaller than the corresponding angle in fluorobenzene (122.27°), calculated at the same level of theory (our data). Furthermore, the $C_6-C_1-C_2$ ring angle in *para*-fluorophenol is also slightly smaller (by about 1.1°) than in phenol, as is shown in Figure 2B (and Table 1). These results clearly indicate that in *p*-fluorophenol, the structural changes of the aromatic ring are governed chiefly by the electronegativity of the fluorine substituent. However, both the OH and F exert their influence on the internal ring angles at the *para*-carbon atoms through the resonance effects. Accordingly, the inductive effect of one substituent (F) increases the internal ring angle at the ipso carbon atom[34,35] while the influence from the other para substituent (OH) leads to a small decrease of this angle, and vice versa.

In Table 1, the interatomic C···C distances in the aromatic ring and the calculated dipole moments of these molecules are also compared. It is evident that the most pronounced changes in the ring geometry are observed for *p*-FPhOH, the $C_1\cdots C_4$ distance decreases by 0.025 Å and the $C_3\cdots C_5$ distance increases by 0.016 Å in *p*-FPhOH relative to phenol.

It is interesting to compare the halogen-substituent effect on the tilt of the phenolic oxygen atom toward the C_1-C_6 bond, which is represented by the angle between the C_1-O bond and the bisector of the $C_6-C_1-C_2$ angle. In phenol, this tilt has been attributed to the repulsion between the hydroxy hydrogen and the adjacent CH hydrogen atoms.[14] As revealed by the calculations at the MP2/6-311++G(df,pd) level, this tilt is equal to 2.72°, 2.82°, and 2.83°, in phenol, *p*-bromo and *p*-chlorophenol, respectively. In the case of *p*-fluorophenol, it has the largest value, 3.25°.

The C_1-O-H bond angle calculated for phenol, 108.11°, is in excellent agreement with the experimental value (108.8° ± 0.4°) from the MW study of phenol vapor.[36] In *p*-halophenols, this angle shows a regular increase in the order F < Cl < Br; however, the change of the OH bond length is negligible (Table 1).

Comparison of the C−H bond lengths in the series of *p*-XPhOH molecules (Table 1) reveals that almost all C−H bonds in *p*-halophenols are shorter than in phenol. In particular, the C_3-H and C_5-H bonds, which are in the vicinity of the electronegative halogen substituent, are significantly shortened, and this effect is most pronounced for fluorine ($\Delta r = -0.0014$ Å). Analysis of the NBO results for *p*-FPhOH has revealed that this is accompanied by the decrease of the occupancies on the antibonding σ^*_{C3-H} and σ^*_{C5-H} orbitals, by about 0.0017e, in comparison to phenol (MP2 electron densities).

Natural Atomic Charges of *p*-XPhOH (X = H, F, Cl, Br). In Figure 3 the natural atomic charges calculated from the NBO analysis for phenol (A), *p*-FPhOH (B), *p*-ClPhOH (C), and *p*-BrPhOH (D) are illustrated. As follows from this comparison, para substitution of phenol with the halogen atom has a negligible effect on the oxygen atom charge. However, it causes a decrease of the positive charge on the C_1 atom. In the case of *p*-fluorophenol, this decrease is most pronounced (by 0.011e). As expected, bonding of an electronegative halogen to the C_4 atom significantly alters the charge on this carbon atom, which ranges from −0.217e in phenol to +0.394e in *p*-fluorophenol. In the latter, a large increase of the charge on C_4 is accompanied by an increase of the negative charges on the C_3 and C_5 atoms, as shown in Figure 3B. Simultaneously, the distance between

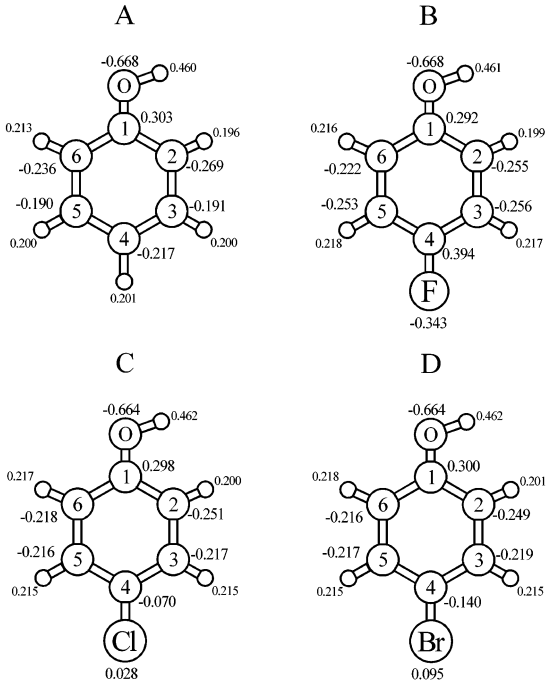

Figure 3. Natural atomic charges calculated for phenol (A); *p*-FPhOH (B); *p*-ClPhOH (C), and *p*-BrPhOH (D). The results from MP2/6-311++G(df,pd) calculations.

the C_3 and C_5 atoms in *p*-FPhOH becomes the largest among all investigated molecules (Table 1). Comparison of the charges on the remaining carbon atoms, C_2 and C_6, reveals the asymmetric distribution of electron density, i.e., the C_2 atom is more negatively charged than the C_6 atom, in each phenol. This is undoubtedly caused by the OH group pointing toward the C_2 atom, as illustrated in Figure 3. Furthermore, the positive charge on the C_2H hydrogen atom is the smallest with respect to other hydrogen atoms.

Infrared Spectra of *p*-Fluorophenol and Its Deuterated (−OD) Derivative. *Comparison with Phenol, p-Chloro- and p-Bromophenol.* The experimental frequencies and integrated infrared intensities of *p*-FPhOH and *p*-FPhOD in inert solvents (cyclohexane and CCl_4) have been measured and are listed in Tables 2 and 3, respectively, together with the harmonic frequencies and infrared intensities of these molecules computed at the B3LYP/6-311++G(df,pd) level. The detailed vibrational assignments of the experimental spectra have been made on the basis of the calculated potential energy distribution (PED). The calculated PED is similar to the results reported recently by Tishchenko et al.[17] for *p*-FPhOH, except for the modes Q13 and Q14. However, in the present work we have also shown the relative phases of atomic displacements, which are very useful in the detailed description of the normal modes. In Figure 4A the infrared spectra of *p*-FPhOH and *p*-FPhOD (measured in CCl_4 solution) are shown in the range from 1500 to 800 cm^{-1}. In Figure 4B the theoretical spectra of these molecules are compared, in the same frequency range. As is seen from this comparison, the calculated frequencies and IR intensities reproduce the experimental spectra very well, which indicates that the reported band assignment is correct.

OH Vibrations. As is seen in Table 2, mode Q2 corresponds to the "pure" torsional vibration of the OH group in *p*-FPhOH, and the predicted frequency of this mode, 289 cm^{-1}, is very similar to the experimental frequency, 279 cm^{-1} (measured in the gas phase).[10] For the deuterated derivative, the OD torsion is also predicted to be a "pure" vibration (Q2 mode in Table 3), and the theoretical frequency, 215 cm^{-1}, is in excellent agreement with experimental 215 cm^{-1}.[10] In our earlier work[1a,8] we have shown that the calculated frequencies of the OH torsional vibration in *p*-chlorophenol (300 cm^{-1}) and *p*-bromophenol (302/311 cm^{-1}) are lower than in phenol (313 cm^{-1}). (All results have been obtained at the B3LYP/6-311++G(df,pd) level.)

As follows from this study, the corresponding OH torsional frequency in *p*-fluorophenol shows the most pronounced red shift with respect to that in phenol. It is interesting to note that the decrease of the OH torsional frequency in *p*-halophenols exactly parallels the lowering of the OH rotational barrier. The experimentally determined 2-fold barrier for OH rotation in phenol, 3.47 kcal/mol, is lowered to 2.88, 3.28, and 3.35 kcal/mol in *p*-fluoro-, *p*-chloro-, and *p*-bromophenol, respectively.[10,31]

According to calculations, the OH in-plane bending vibration, δ(OH), in *p*-FPhOH predominantly contributes to the mode Q20. This mode has a large theoretical infrared intensity (Table 2). Thus, mode Q20 can be assigned to the very intense band at 1174 cm^{-1}. As illustrated in Figure 4A, this band disappears in the spectrum of the OD deuterated counterpart, which supports our assignment. In the experimental spectrum of *p*-FPhOH (Figure 4A) there is, however, an additional weak shoulder at 1196 cm^{-1} (which is observed as a distinct band at 1192 cm^{-1} in the spectrum of *p*-FPhOD). According to the theoretical results, no other fundamental should occur in this frequency range, except for the normal mode Q21, which has very large infrared intensity. Therefore, the strong band observed at 1226 cm^{-1} has been assigned to Q21 (this mode involves a main contribution from the C−F stretching vibration), while the weak shoulder at 1196 cm^{-1} is assigned to a combination tone. Among the possible combinations, the most plausible are $458_{Q7} + 747_{Q11} = 1205$ cm^{-1} or $445_{Q6} + 747_{Q11} = 1192$ cm^{-1}, which interact by Fermi resonance with the fundamental transition, Q21. The fundamental and the possible combination tones have the same symmetry (A′), which fulfils the resonance conditions. The combination band gains substantial infrared intensity at the expense of the fundamental. In such a case, the experimental infrared intensity of Q21 is lower than the theoretically calculated intensity in the harmonic approximation. We have shown in our earlier studies on phenol[1b] that the absorption pattern in the range 1200−1160 cm^{-1} is strongly affected by multiple anharmonic resonances.

In *p*-fluorophenol the OH in-plane bending vibration also contributes to the mode Q24 (20%) assigned at 1323 cm^{-1}, and to the mode Q25 (11%) at 1437 cm^{-1} (Table 2). All these bands are sensitive to the deuteration of the phenolic OH group (as shown in Figure 4A and in Table 3). It should be emphasized that the corresponding bands in the spectra of other *p*-halophenols have been observed at very similar frequencies: 1176, 1320, and 1424 cm^{-1} for *p*-ClPhOH and 1176, 1320, and 1423 cm^{-1} for *p*-BrPhOH,[8] whereas for phenol, these bands occur at 1179 and 1341 cm^{-1}.[1a]

In the IR spectrum of *p*-FPhOD, a new doublet appears at 914 and 936 cm^{-1}, as illustrated in Figure 4A. According to calculations (Table 3), only one normal mode (Q16) should be observed in this region, since the next mode, Q17, has zero IR intensity. It is interesting to note that an analogous doublet is also observed in the IR spectra of *p*-ClPhOD (918 and 938 cm^{-1}) and *p*-BrPhOD (918 and 939 cm^{-1}, our data). On the contrary, only one band, at 920 cm^{-1}, was observed in the IR spectrum of PhOD, and it was assigned to the OD in-plane bending vibration, δ(OD).[1a] These data indicate that in *p*-XPhOD (X = F, Cl, Br) the in-plane OD bending vibration (Q16 mode, *A*′ symmetry) enters into Fermi resonance (FR) with

TABLE 2: Vibrational Frequencies (cm^{-1}), IR Intensities (km·mol^{-1}) and Band Assignments for *p*-Fluorophenol-OH (*p*-FPhOH)

		experimental values			B3LYP/6-311++G(df, pd)		
	sym	ν[a]	A	I_{rel}[b]	ω[c]	A	PED[%][d]
Q1	A″				153	0	$\tau_3$ring(62), $\tau_2$ring(22)
Q2	A″	279[e]			289	112	τOH(100)
Q3	A′	345[e]			339	6	δCF(+43), δCO(−41)
Q4	A″	371[f]			361	0	$\tau_1$ring(40), γCF(+37), γCO(−23)
Q5	A″				422	1	$\tau_2$ring(76), $\tau_3$ring(24)
Q6	A′	445	2.5	6	442	6	δCF(+36), δCO(+36), $\delta_3$ring(23)
Q7	A′	458	0.8	2	457	1	$\delta_2$ring(73)
Q8	A″	509	11.5	28	507	23	γCO(+33), γCF(+22), $\tau_3$ring(22)
Q9	A′	640	0.1	0	644	1	$\delta_3$ring(69)
Q10	A″	696	0.2	0	667	0	$\tau_1$ring(71), γCO(+17), γCF(−11)
Q11	A′	747	27.1	67	744	66	$\delta_1$ring(35), ν(CF)(+22), ν(CO)(−20)
Q12	A″	792	1.3	3	791	11	γC_2H(+52), γC_3H(+27), γC_5H(−10), γC_6H(−10)
Q13	A″	828	30.2	74	828	63	γC_6H(+39), γC_5H(+27), γC_2H(+12), γCO(−13), γCF(−9)
Q14	A′	851	0.2	0	850	0	ν(CC)(61), $\delta_2$ring(15)
Q15	A″	879	1.4	3	899	3	γC_3H(+59), γC_2H(−29), γC_5H(+12)
	A′	916	0.1				overtone ($2 \times 458_{Q7}$)
Q16	A″	942[f]			942	0	γC_5H(+47), γC_6H(−43), γC_3H(−10)
Q17	A′	1011	0.3	1	1011	1	ν(CC)(45), $\delta_1$ring(38)
Q18	A′	1088	7.4	18	1096	20	δC_5H(+20), δC_3H(+16), $\nu(C_5C_6)$(−16), $\nu(C_2C_3)$(+14)
Q19	A′	1149	1.6	4	1155	2	δC_3H(+27), δC_5H(−20), δC_2H(−16), δC_6H(+15)
Q20	A′	1174	63.0	155	1167	149	δOH(+56), $\nu(C_1C_6)$(−15), δC_6H(+9)
	A′	1196					combination[g]
Q21	A′	1226	45.5	112	1221	180	ν(CF)(−40), $\delta_1$ring(18), δC_2H(−11), δC_6H(+10)
Q22	A′	1262	6.5	16	1265	21	ν(CO)(−46), $\nu(C_5C_6)$(+12), $\nu(C_2C_3)$(+11) ν(CF)(−8)
Q23	A′	1310	1.9	5	1299	2	δC_2H(−19), δC_6H(−15),δC_5H(−14), δC_3H (−12), $\nu(C_3C_4)$(+15)
Q24	A′	1323	7.0	17	1335	26	ν(CC)(53), δOH(+20), δC_5H(−14), δC_3H(−11)
Q25	A′	1437	10.4	25	1446	27	$\nu(C_5C_6)$(+20), $\nu(C_2C_3)$(−16), δC_6H(−13), δOH(+11)
Q26	A′	1510	97.5	239	1519	237	δC_2H(−16), δC_6H(+10), δC_5H(+12),δC_3H (−11), $\nu(C_3C_4)$(−12)
Q27	A′	1603	0.3	1	1618	3	$\nu(C_4C_5)$(+26), $\nu(C_1C_2)$(+23)
Q28	A′	1611	0.2	0	1629	0	$\nu(C_1C_6)$(+18), $\nu(C_3C_4)$(+18), $\nu(C_5C_6)$(−16), $\nu(C_2C_3)$(−16)
Q29	A′	3035	2.1	5	3029	12	$\nu(C_2-H)$(97)
Q30	A′	3052	0.7	2	3060	3	$\nu(C_6H)$(+57), $\nu(C_5H)$(−43)
Q31	A′	3065	0.6	1	3069	1	$\nu(C_3-H)$(95)
Q32	A′	3077	0.3	1	3073	1	$\nu(C_5H)$(+55), $\nu(C_6H)$(+43)
Q33	A′	3613	55.5	136	3658	64	ν(O−H)(100)

[a] From the IR spectra of cyclohexane and CCl_4 solutions (this work) otherwise as indicated. [b] I_{rel}, integral absorbances of absorption bands normalized in such a way that the observed intensity sum of all bands is equal to the B3LYP-calculated intensity sum of the corresponding modes. [c] The scaling factor for frequencies was 0.983, except for modes Q29−Q32 (0.958) and Q33 (0.954), see text. [d] Predominant contributions (those below 10% are summarized and given as a total). Abbreviations: ν, stretching; δ, in-plane bending; γ, out-of-plane bending; τ, torsional vibration. The phases of the internal coordinates are indicated by signs: the plus sign corresponds to the clockwise in-plane bending, or the in-phase stretching (or the out-of-plane bending) vibrations, the minus sign has the opposite meaning. [e] Ref 10 (gas-phase data). [f] Ref 12 (Raman data, solid). [g] Combination tone, see text.

a combination tone of the same symmetry. The most probable is the following combination: $509_{Q8} + 421_{Q5} = 930$ cm^{-1} (A″ × A″ = A′). From the measured frequencies and infrared intensities of both the bands, we have estimated their unperturbed frequencies.[37] These values are 924 and 926 cm^{-1} for the combination and the fundamental tone (Q16). Thus, the combination band is red-shifted while the δ(OD) band is blue-shifted, each by 10 cm^{-1}. Moreover, the IR intensity of the latter band significantly decreases, as shown in Table 3.

The O−H stretching vibration in *para*-fluorophenol is observed at 3613 cm^{-1} (in CCl_4 solution), which is in accordance with the data reported by Cabana et al.[11] It should be stressed, however, that the calculated frequency of the ν(OH) vibration, 3658 cm^{-1}, exactly reproduces the experimental frequency of *p*-FPhOH in the vapor phase, 3658 cm^{-1} (NIST Chemistry Web-Book). The former frequency has been calculated from the B3LYP-harmonic frequency by using the scale factor of 0.953. In our earlier theoretical studies of phenol[1a] we have shown that the harmonic frequency of ν(OH) calculated at the B3LYP/6-311++G(df,pd) level and scaled by 0.953 gives excellent agreement with the experimental anharmonic frequency of phenol in the vapor phase.

It is worth mentioning that the theoretical O−H stretching frequency in *p*-fluorophenol is slightly higher (by 4 cm^{-1}) than that computed for phenol, and this is supported by experimental data.[11] As shown in Table 1, the O−H bond in *p*-FPhOH is slightly shortened. These results consistently indicate that the O−H bond in *p*-FPhOH is a little stronger than that in the parent phenol.

C−F Vibrations. The ν(C−F) stretching vibration contributes predominantly to the very strong absorption at 1226 cm^{-1} (mode Q21, discussed earlier) and to the strong band at 747 cm^{-1} (mode Q11). It should be noted that in the IR spectrum of fluorobenzene, the C−F stretching vibration was assigned to the very strong band at 1238 cm^{-1}.[38] The calculated infrared intensities of the modes Q21 and Q11 in *p*-FPhOH are quite large. It is interesting to note that two analogous bands (though of much lower intensities) have been observed in the IR spectra of *p*-ClPhOH and *p*-BrPhOH (1096 cm^{-1}, 644 cm^{-1}) and (1071 cm^{-1}, 606 cm^{-1}), respectively.[8]

According to the calculated PED, the out-of-plane γ(CF) and γ(CO) vibrations are strongly mixed and contribute mainly to the Q4 and Q8 modes and, to some extent, to Q13 (Table 2). As is seen in Figure 3 for *p*-fluorophenol (B), the negative charges are accommodated on both the oxygen and fluorine atoms (−0.668e and −0.343e, respectively). In the case of mode

TABLE 3: Vibrational Frequencies (cm^{-1}), IR Intensities (km·mol^{-1}), and Band Assignments for *p*-Fluorophenol-OD (*p*-FPh-OD)

		experimental values			B3LYP/6-311++G(df, pd)		
	sym	ν[a]	A	I_{rel}[b]	ω [c]	A	PED[%][d]
Q1	A″				150	0	$\tau_3$ring(60), $\tau_2$ring(21)
Q2	A″	215[e]			215	60	τOD(96)
Q3	A′	334[e]			329	7	δCO(−48), δCF(+35)
Q4	A″				360	0	$\tau_1$ring(40), γCF(+37), γCO(−23)
Q5	A″				421	0	$\tau_2$ring(76), $\tau_3$ring(24)
Q6	A′	436	2.2	7	432	7	δCF(+43), δCO(+28), $\delta_3$ring(19)
Q7	A′	455	0.1	0	454	0	$\delta_2$ring(71)
Q8	A″	509	10.1	31	506	20	γCO(+33), $\tau_3$ring(23), γCF(+22)
Q9	A′	639	0.2	1	642	1	$\delta_3$ring(71)
Q10	A″	684	0.6	2	667	0	$\tau_1$ring(71), γCO(+17), γCF(−11)
Q11	A′	742	17.2	53	739	53	$\delta_1$ring(35), n(CF)(+21), n(CO)(−20)
Q12	A″	792	1.6	5	791	10	γC_2H(+52), γC_3H(+27), γC_5H(−11), γC_6H(−10)
Q13	A″	830	28.6	89	828	66	γC_6H(+38), γC_5H(+27), γC_2H(+13), γCO(−13), γCF(−9)
Q14	A′	853	1.1	3	846	7	n(CC)(58), $\delta_2$ring(16), n(CF)(+11)
Q15	A″	870	0.8	2	899	3	γC_3H(+59), γC_2H(−29), γC_5H(+12)
		914	8.6				combination ($509_{Q8} + 421_{Q5}$)
Q16	A′	936	10.5	37	915	78	δOD(+80), n(C_1C_2)(+10)
Q17	A″				942	0	γC_5H(+47), γC_6H(−43), γC_3H(−10)
Q18	A′	1010	0.3	1	1011	1	$\delta_1$ring(41), n(CC)(40), δCH(19)
Q19	A′	1091	5.2	16	1102	15	δC_5H(+19), δC_6H(−18), n(C_5C_6)(−15), $\delta_3$ring(+15)
Q20	A′	1149	0.4	1	1155	1	δC_3H(+27), δC_5H(−20), δC_2H(−16), δC_6H(+15)
		1192					combination[g]
Q21	A′	1226	59.4	185	1221	210	ν(CF)(−39), $\delta_1$ring(19), δC_6H(+12), δC_2H(−10)
Q22	A′	1255	9.7	30	1258	32	ν(CO)(−46), ν(C_2C_3)(+15), ν(C_5C_6)(+11), ν(CF)(−10)
Q23	A′	1282	0.2	1	1299	2	δC_2H(−23),δC_6H(−18),δC_5H(−17),δC_3H(−16),ν(C_3C_4)(+10)
Q24	A′	1294	2.0	6	1310	7	ν(C_1C_2)(+22), ν(C_1C_6)(−18), ν(C_3C_4)(+13), ν(C_4C_5)(−11)
Q25	A′	1423	2.4	7	1432	4	ν(C_5C_6)(+23), ν(C_2C_3)(−21), δC_6H(−10)
Q26	A′	1508	85.2	265	1517	264	δC_2H(−15),δC_5H(+13),δC_6H(+12), δC_3H(−12),ν(C_3C_4)(−10)
Q27	A′	1601	0.1	0	1613	1	ν(C_4C_5)(−25), ν(C_1C_2)(−22), ν(C_3C_4)(+14), ν(C_1C_6)(+12)
Q28	A′	1624	0.1	0	1628	2	ν(C_5C_6)(+20), ν(C_2C_3)(+18), ν(C_3C_4)(−13), ν(C_1C_6)(−13)
Q29	A′	2668	31.7	98	2663	40	ν(OD)(100)
Q30	A′	3047	2.9	9	3029	13	ν(C_2H)(97)
Q31	A′	3052	0.3	1	3060	3	ν(C_6H)(+57), ν(C_5H)(−43)
Q32	A′	3066	0.1	0	3069	1	ν(C_3H)(95)
Q33	A′	3078	0.1	0	3073	1	ν(C_5H)(+55), ν(C_6H)(+43)

[a] From the IR spectra of cyclohexane and CCl_4 solutions (this work) otherwise as indicated. [b] I_{rel}, integral absorbances of absorption bands normalized in such a way that the observed intensity sum of all bands is equal to the B3LYP-calculated intensity sum of the corresponding modes. [c] The scaling factor for theoretical frequencies was 0.983, except for mode Q29 (0.954) and Q30−Q33 (0.958), see text. [d] Predominant contributions (those below 10% are summarized and given as a total). Abbreviations: ν, stretching; δ, in-plane bending; γ, out-of-plane bending; τ, torsional vibration. The phases of the internal coordinates are indicated by signs: the plus sign corresponds to the clockwise in-plane bending, or the in-phase stretching (or the out-of-plane bending) vibrations, the minus sign has the opposite meaning. [e] Ref 10 (gas-phase data). [f] Ref 12 (Raman data, solid). [g] Combination tone, see text.

Q8, the simultaneous out-of-plane and in-phase motion of the O and F atoms causes considerable changes of the molecular dipole moment, the same concerns mode Q13. Therefore, the corresponding bands in the IR spectrum are quite strong. Conversely, mode Q4 involving the out-of-phase γ(CF) and γ-(CO) vibrations has zero theoretical IR intensity, as shown in Table 2. Therefore, this mode is not observed in infrared (but it appears in the Raman spectrum[12]).

C−O Vibrations. In the IR spectrum of *p*-FPhOH, the weak band at 1262 cm^{-1} is slightly shifted upon deuteration (Figure 4A) and it involves predominant contribution from the ν(C−O) stretching vibration (mode Q22). Such a small intensity of this band is quite striking in comparison to the corresponding band in phenol, at 1257 cm^{-1}.[1a] This effect is supported by the theoretical results; the predicted infrared intensity of mode Q22 is equal to only 21 km/mol, whereas in phenol, the calculated intensity of this mode amounts to 90 km/mol (at the same level of theory). In *para*-chlorophenol and *para*-bromophenol the calculated IR intensities of the corresponding modes are even larger, $A = 108$ and 126 km/mol, respectively, and these results are supported by the experimental data.[8] Such a quenching of the IR intensity of the mode Q22 in *p*-FPhOH is worth some comment. As follows from Table 2, this normal mode can be described as a simultaneous contracting of the C−O bond and stretching of the C_5-C_6 and C_3-C_2 bonds (also the C−F bond slightly contracts). As follows from Figure 3, the negative charge on the oxygen atom has approximately the same value in all phenols; however, the charges on the C_3 and C_5 carbon atoms in *p*-fluorophenol are much more negative than those in other molecules. Thus, it can be concluded that in *p*-FPhOH, the resultant change of the dipole moment during this coupled vibration is very small. Consequently, this causes a quenching of the IR intensity of the corresponding band.

C−H and Phenyl Ring Vibrations. The frequencies of the observed C−H stretching vibrations have been obtained from resolving the bands in the frequency range 2900−3100 cm^{-1} and are listed in Tables 2 and 3. According to the calculations, mode Q29 corresponds to pure C_2-H stretching in *p*-FPhOH (Table 2) and gives rise to the band of the largest IR intensity and lowest frequency. This can be related to the fact that the calculated C_2-H atom distance in *p*-fluorophenol is longer, by about 0.003 Å than other C−H bond lengths (Table 1). Also, the charge on this hydrogen atom is the smallest of all hydrogen atoms, as discussed earlier. According to the theoretical results obtained for phenol and other halogenophenols, the pure C_2-H stretching vibration has always been detected in the spectra as

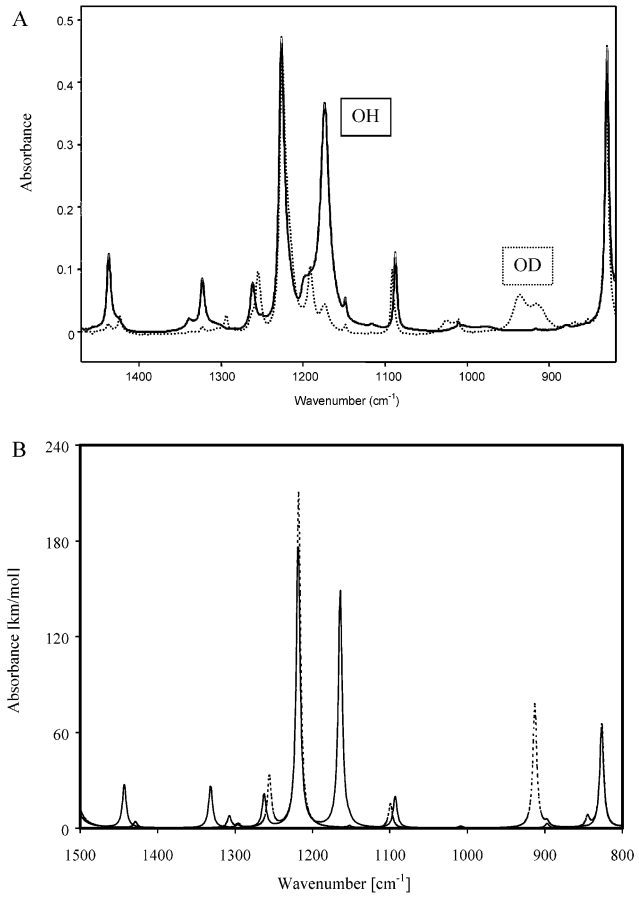

Figure 4. (A) Infrared spectra of *p*-fluorophenol (solid line) and its OD-deuterated derivative (dotted line) in CCl_4 solution ($c = 0.05$ mol dm^{-3}, and path length = 0.04 cm). (B) Theoretical IR spectra of these molecules calculated with the B3LYP method and 6-311++G(df,pd) basis set. (In the simulated spectra the Lorentz function and the half bandwidth of 5 cm^{-1} have been used.)

the most intense band of the lowest frequency, among all C−H stretching vibrations.[1a,8] Therefore, for *p*-fluorophenol, we can assign the strongest infrared band centered at 3035 cm^{-1} to the $\nu(C_2-H)$ vibration. The predicted frequency of this mode, 3029 cm^{-1}, is only 6 cm^{-1} lower than experimental. In the IR spectrum this band is slightly asymmetric, which is probably caused by the presence of the first overtone of the Q26 mode ($2 \times 1510 = 3020$ cm^{-1}). In addition, two possible combinations, i.e., $1437_{Q25} + 1611_{Q28}$ and $1437_{Q25} + 1603_{Q27}$ may affect the absorption pattern of the C−H stretching vibrations (the detailed analysis of these transitions in phenol and halophenols, in the frequency range of 2900−3100 cm^{-1}, will be reported elsewhere).

The band observed at 3065 cm^{-1} (calcd. 3069) in the spectrum of *p*-FPhOH has been assigned to the pure $\nu(C_3-H)$ stretching vibration, as revealed by the calculated PED. It is interesting to note that in *p*-chloro- and *p*-bromophenol as well as in their OD-deuterated derivatives the $\nu(C_3-H)$ stretch is also an isolated vibration,[8] while in parent phenol it is strongly coupled with $\nu(C_5-H)$.[1a] This indicates that the halogen substituent in the para position of the phenyl ring alters the coupling between the C−H stretching vibrations. The remaining two bands observed at 3077 and 3052 cm^{-1} have been assigned to the coupled $\nu(C_5-H)$ and $\nu(C_6-H)$ stretchings (in-phase, and out-of-phase motions, respectively). We have shown earlier[1a] that the use of the scaling factor of 0.958 for the B3LYP-calculated C−H stretching frequencies almost reproduces the experimental anharmonic frequencies. It should be mentioned that this factor for frequencies has been derived from the scaling factor for the valence CH stretching force constant (0.918) reported by Pulay and co-workers.[26]

The C−H bending vibrations in *p*-FPhOH and *p*-FPhOD are strongly coupled with ring deformations and contribute to several bands in the range from 790 to 1510 cm^{-1}. The detailed vibrational assignment is shown in Tables 2 and 3, and we shall discuss only the most characteristic features in this range of the spectrum. According to the calculations, mode Q26 has the largest IR intensity (237 km/mol). The theoretical frequency of this mode, 1519 cm^{-1}, corresponds very well to the experimental frequency (1510 cm^{-1}) of the strongest band in the spectrum of *p*-FPhOH. For the OD-counterpart, the analogous very strong band is observed at 1508 cm^{-1}. The calculated PED has revealed that mode Q26 arises from the coupling between the in-plane CH bending and CC stretching vibrations. Examination of the phases of the internal coordinates indicates that during this normal mode the total dipole moment changes substantially, and this is consistent with the large IR intensity of this mode. In contrast, extremely low IR intensity has been predicted for the mode Q23 (observed at 1310 cm^{-1}). This mode involves almost the same internal coordinates, but in different phases (Table 2). It is worth noting that in the IR spectra of *p*-chloro- and *p*-bromophenol the bands positioned at 1494 and 1489 cm^{-1}, respectively, have the highest intensity,[8] while in phenol the corresponding band at 1499 cm^{-1} is much weaker.[1a]

The characteristic band observed at 828 cm^{-1} in the spectrum of *p*-FPhOH is attributed to the mode Q13 (the calculated frequency reproduces the experimental, as shown in Table 2). This band arises from the coupled out-of-plane CH vibrations and is commonly used to identify para substitution in the benzene ring.

The other characteristic feature of the infrared spectrum of *p*-FPhOH is the extremely low intensity of the bands corresponding to the ring-puckering mode Q10 (at 696 cm^{-1}) and those arising from the C−C stretching vibrations in the aromatic ring (modes Q27 and Q28 at 1603 and 1611 cm^{-1}, respectively). These bands almost disappear from the IR spectra of *p*-fluorophenol. The theoretically predicted IR intensities of these modes (0, 3, and 0 km/mol, respectively) confirm the experimental results. It should be emphasized that in phenol, the corresponding modes (designated as 4, 8a, and 8b, by analogy to benzene) generate the bands at similar frequencies (689, 1598, and 1606 cm^{-1}, respectively) but their intensities are quite large.[1a] The forms of these normal modes in PhOH and *p*-FPhOH are very similar, as revealed by the PEDs calculated for both the molecules, therefore, the differences in infrared intensities should be attributed to some other factors. As illustrated in Figure 3, atom C_4 in phenol has a negative charge, whereas in *p*-fluorophenol it gains a large positive charge (0.394e). Moreover, in *p*-FPhOH, the C_3 and C_5 atoms acquire large negative charges and simultaneously the interatomic $C_3 \cdots C_5$ distance becomes the largest, whereas the $C_1 \cdots C_4$ distance becomes the smallest, as compared to other phenols. It is known that during the normal mode involving several internal coordinates, the individual contributions to the total change of the dipole moment (determined by the phases of these coordinates) can cancel themselves. Consequently, this causes a large drop in the IR intensity of this mode. Such effects are observed in the case of *p*-FPhOH.

Thus, significant structural changes and redistribution of atomic charges in the phenol ring, caused by the fluorine substituent in the para position, manifest themselves in the

unusual intensity pattern of the bands corresponding to ring stretching and ring puckering modes in *p*-fluorophenol.

Concluding Remarks

The most important conclusions from this study can be summarized as follows. (1) In *para*-fluorophenol, the structural changes of the aromatic ring are governed chiefly by the electronegativity of fluorine (inductive effect). However, the resonance effects caused by the OH and F substituents in the para position also contribute to the geometrical changes of the ring. Accordingly, the inductive effect of one substituent (F) increases the internal ring angle at the ipso carbon atom, while the influence from the other para substituent (OH) leads to a small decrease of this angle, and vice versa. (2) In *p*-ClPhOH and *p*-BrPhOH some quinoid-type structure of the ring is apparent. (3) The natural atomic charges calculated for *p*-XPhOH (X = H, F, Cl, Br) have revealed interesting information on the charge distribution in the phenol ring. The charge on the C_1 atom (in para position to halogen) regularly decreases in the order H > Br > Cl > F. It should be mentioned that this decrease parallels the decrease of the OH torsional frequency (as well as the experimentally determined OH rotational barrier in these phenols). (4) The harmonic frequencies and infrared intensities of *p*-fluorophenol and its OD- deuterated derivative calculated with the B3LYP method and 6-311++G(df,pd) basis set are in excellent agreement with the experimental IR data. (5) A striking quenching of the IR intensity of the bands corresponding to the ring stretching and ring puckering modes in the title molecule (in particular, of the bands around 1610 cm^{-1}) is attributed to canceling of the dipole moment changes during these coupled vibrations. This, in turn, is the consequence of significant structural changes and redistribution of atomic charges in the phenol ring, caused by the fluorine substituent in the para position. (6) The unequivocal assignment of the bands in the infrared spectrum of a title molecule can be used in a further study of the hydrogen-bonded complexes and clusters of *para*-fluorophenol.

Acknowledgment. The generous computer time from the Poznań Supercomputer and Networking Center as well as Wrocław Supercomputer and Networking Center is acknowledged. This research has been supported by Polish Committee for Scientific Research (KBN Grants: 4T09A11922 and 7T09A 00821).

Supporting Information Available: Table containing the results from the B3LYP/6-311++G(df,pd) calculations of geometrical parameters of *p*-XPhOH (X=H, F, Cl, Br). This material is available free of charge via the Internet at http://pubs.acs.org.

References and Notes

(1) (a) Michalska, D.; Zierkiewicz, W.; Bieńko, D. C.; Wojciechowski, W.; Zeegers-Huyskens, T. *J. Phys. Chem. A* **2001**, *105*, 8734. (b) Michalska, D.; Bieńko, D. C.; Abkowicz-Bieńko, A. J.; Latajka, Z. *J. Phys. Chem.* **1996**, *100*, 17786.

(2) Keresztury, G.; Billes, F.; Kubinyi, M.; Sundius, T. *J. Phys. Chem. A* **1998**, *102*, 1371.

(3) Lampert, H.; Mikenda, W.; Karpfen, A. *J. Phys. Chem. A* **1997**, *101*, 2254.

(4) Grafton, A. K.; Wheeler, R. A. *J. Comput. Chem.* **1998**, *19*, 1663.

(5) (a) Schiefke, A.; Deusen, C.; Jacoby, C.; Gerhards, M.; Schmitt, M.; Kleinermanns, K.; Hering, P. *J. Chem. Phys.* **1995**, *102*, 9197. (b) Roth, W.; Imhof, P.; Gerhards, M.; Schumm, S.; Kleinermanns, K. *Chem. Phys.* **2000**, *252*, 247.

(6) Re, S.; Osamura, Y. *J. Phys. Chem. A* **1998**, *102*, 3798.

(7) Hobza, P.; Burcl, R.; Špirko, V.; Dopfer, O.; Müller-Dethlefs, K.; Schlag, E. W. *J. Chem. Phys.* **1994**, *101*, 990.

(8) Zierkiewicz, W.; Michalska, D.; Zeegers-Huyskens, T. *J. Phys. Chem. A* **2000**, *104*, 11685.

(9) Cabana, A.; Patenaude, J. T.; Sandorfy, C.; Bavin, P. M. *J. Phys. Chem.* **1960**, *64*, 1941.

(10) Larsen, N. W.; Nicolaisen, F. M. *J. Mol. Struct.* **1974**, *22*, 29.

(11) Jakobsen, R. J.; Brewer, E. J. *Appl. Spectrosc.* **1962**, *16*, 32.

(12) Green, J. H. S.; Harrison, D. J.; Kynaston, W. *Spectrochim. Acta* **1971**, *27A*, 2199.

(13) Vajda, E.; Hargittai, I. *J. Phys. Chem.* **1993**, *97*, 70.

(14) Kovács, A.; Macsári, I.; Hargittai, I. *J. Phys. Chem. A* **1999**, *103*, 3110.

(15) Macásri, I.; Izvekov, V.; Kovács, A. *Chem. Phys. Lett.* **1997**, *269*, 393.

(16) Remmers, K.; Meerts, W, L. Zehnacker-Rentien, A.; LeBarbu, K.; Lahmani, F. *J. Chem. Phys.* **2000**, *112*, 6237.

(17) Tishchenko, O.; Kryachko, E. S.; Nguyen, M. T. *Spectrochim. Acta A* **2002**, *58*, 1951.

(18) (a) Brzezinski, B.; Brycki, B.; Zundel, G.; Keil, T. *J. Phys. Chem.* **1991**, *95*, 8598. (b) Keil, T.; Brzezinski, B.; Zundel, G. *J. Phys. Chem.* **1992**, *96*, 4421.

(19) Ouvrard, C.; Berthelot, M.; Laurence, C. J. *Chem. Soc., Perkin Trans.* **1999**, *2*, 1357.

(20) Möller, C.; Plesset, M. S. *Phys. Rev.* **1934**, *46*, 618.

(21) (a) Becke, A. D. *J. Chem. Phys.* **1993**, *98*, 5648. (b) Becke, A. D. *J. Chem. Phys.* **1996**, *104*, 1040.

(22) Lee, C.; Yang, W.; Parr, R. G. *Phys. Rev. B* **1988**, *37*, 785.

(23) Krishnan, R.; Binkley, J. S.; Seeger, R.; Pople, J. A. *J. Chem. Phys.* **1980**, *72*, 650.

(24) Frisch, M. J.; Pople, J. A.; Binkley, J. S. *J. Chem. Phys.* **1984**, *80*, 3265.

(25) Reed, A. E.; Curtiss L. A.; Weinhold, F. *Chem. Rev.* **1988**, *88*, 899.

(26) Baker, J.; Jarzecki, A. A.; Pulay, P. *J. Phys. Chem. A* **1998**, *102*, 1412.

(27) Fogarasi, G.; Pulay, P. In *Vibrational Spectra and Structure*; Durig, J. R., Ed., Elsevier: New York, 1985; Vol. 13.

(28) Nowak, M. J.; Lapinski, L.; Bieńko, D. C.; Michalska, D. *Spectrochim. Acta A* **1997**, *53*, 855.

(29) Bieńko, D. C.; Michalska, D.; Roszak, S.; Wojciechowski, W.; Nowak, M. J.; Lapinski, L. *J. Phys. Chem. A.* **1997**, *101*, 7834.

(30) Frisch, M. J.; Trucks, G. W.; Schlegel, H. B.; Scuseria, G. E.; Robb, M. A.; Cheeseman, J. R.; Zakrzewski, V. G.; Montgomery, J. A.; Stratmann, R. E.; Burant, J. C.; Dapprich, S.; Millam, J. M.; Daniels, A. D.; Kudin, K. N.; Strain, M. C.; Farkas, O.; Tomasi, J.; Barone, V.; Cossi, M.; Cammi, R.; Mennucci, B.; Pomelli, C.; Adamo, C.; Clifford, S.; Ochterski, J.; Petersson, G. A.; Ayala, P. A.; Cui, Q.; Morokuma, K.; Malick, K. D.; Rabuck, A. D.; Raghavachari, K.; Foresman, J. B.; Cioslowski, J.; Ortiz, J. V.; Stefanov, B. B.; Liu, G.; Liashenko, A.; Piskorz, P.; Komaromi, I.; Gomperts, R.; Martin, R. L.; Fox, D. J.; Keith, T.; Al.-Laham, M. A.; Peng, C. Y.; Nanayakkara, A.; Gonzales, C.; Challacombe, M.; Gill, P. M. W.; Johson, B. G.; Chen, W.; Wong, M.; Anders, J. L.; Head-Gordon, M.; Replogle, E. S.; Pople, J. A. *Gaussian 98*, rev A1; Gaussian, Inc.: Pittsburgh, PA, 1998.

(31) Larsen, N. W. *J. Mol. Struct.* **1986**, *144*, 83.

(32) Nygaard, L.; Bojesen, I.; Pedersen, T.; Rastrup-Andersen, J. *J. Mol. Struct.* **1968**, *2*, 209.

(33) Hargittai, M.; Hargittai, I. *Int. J. Quantum Chem.* **1992**, *44*, 1057.

(34) Portalone, G.; Schultz, G.; Domenicano, A.; Hargittai, I. *Chem. Phys. Lett.* **1992**, *197*, 482.

(35) Krygowski, T. M. In *Progress in Physical Organic Chemistry*; Taft, R. W., Ed.; John Wiley: New York, 1990; Vol. 17 p 239, and references therein.

(36) Larsen, N. W. *J. Mol. Struct.* **1979**, *51*, 175.

(37) Miyazawa, T. *J. Mol. Spectrosc.* **1960**, *4*, 168.

(38) Lipp, E. D.; Seliskar, C. J. *J. Mol. Spectrosc.* **1981**, *87*, 255.